

Experiment on Erbium-Doped Fiber Amplifiers

Li Qian*

Advanced Labs for Special Topics in Photonics (ECE 1640H)

University of Toronto

April 28, 1998

1. Purpose of the Experiment

- Understand the principle of operation of the erbium-doped fiber amplifier (EDFA).
- Construct an EDFA and an erbium-doped fiber laser.
- Measure and calculate the essential parameters of the constructed EDFA.

2. Basic Theory

The basic theories on optical amplification by erbium-doped fibers are presented in this section as preparation for the discussions on noise characteristics and noise reduction methods presented in the next two sections. Many essential terms such as population inversion factor, gain and saturation are explained and defined here for later discussions.

* We gratefully acknowledge Li Qian for her permission to use her student report on our Web site. Li wrote this report while taking the Advanced Topics in Photonics course at the University of Toronto. She is currently Assistant Professor in the Department of Electrical and Computer Engineering at the University of Toronto.

2.1 The Three-level Pumping Scheme

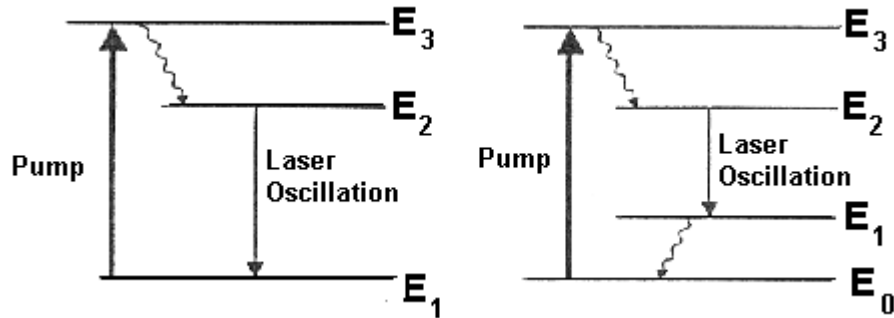


Fig. 1. Schematic illustration of (a) three-level and (b) four-level pumping schemes. Wavy arrows indicate fast relaxation of the level population through nonradiative processes. [After Ref. 1].

Optical amplifiers amplify incident light through stimulated emission, the same mechanism used by lasers. In the case of erbium-doped fibers, the optical gain is supplied by the excited erbium ions (Er^{3+}) when the amplifier is pumped to achieve population inversion. Depending on the energy states of the dopant, pumping schemes can be classified as a three- or four-level scheme (Figure 1). In both cases dopants are excited to a higher energy state through absorption of pump photons and then relax rapidly to a lower excited state (state 2). The stored energy is then used to amplify a signal beam through stimulated emission; thereby energy is transferred from the pump to the signal. The main difference between the three- and four-level pumping schemes is related to the energy state occupied by the dopant after the stimulated-emission event. In the case of a three-level scheme, the lower level is the ground state, whereas it is an excited state with a fast relaxation time in the four-level scheme. It is this difference that necessitates stronger pumping with the 3-level scheme in order to achieve a population inversion, as will be seen later. Erbium-doped fiber amplifiers make use of the three-level pumping scheme.

Rate Equations

To study the behavior of this 3-level system, a rate-equation approach is used to relate the various processes (spontaneous and stimulated emission, absorption, pumping) to the population in the three states.

The following processes contribute to the population (N_1) in state 1:

- Spontaneous emission from state 2 with a time constant τ_{21} .
- Stimulated emission from state 2 for amplification of the signal at a rate of W_s , which depends on the signal photon flux.
- Stimulated emission from E_3 at a rate W_p , which depends on the pump photon flux.

The following processes depopulate state 1:

- Pumping (absorption of the pump photons) at the rate W_p .
- Absorption of the signal photons at the rate W_s .

Therefore, the rate equation for the population in state 1 is

$$\frac{dN_1}{dt} = \frac{N_2}{\tau_{21}} + W_s (N_2 - N_1) - W_p (N_1 - N_3). \quad (1)$$

Similarly we can write the rate equations for the other two states:

$$\frac{dN_2}{dt} = \frac{N_3}{\tau_{32}} - \frac{N_2}{\tau_{21}} - W_s (N_2 - N_1), \quad (2)$$

$$\frac{dN_3}{dt} = -\frac{N_3}{\tau_{32}} + W_p (N_1 - N_3). \quad (3)$$

Steady-state Population Inversion Factor

In order to obtain gain, the stimulated emission from state 2 to state 1 must be greater than the absorption from state 1 to state 2. This condition implies that the population in state 2 must be maintained at a greater level than that of state 1, i.e. population inversion. The degree of population inversion is expressed by the *population inversion factor*¹ n_{sp}

$$n_{sp} \equiv \frac{N_2}{N_2 - N_1}. \quad (4)$$

At steady-state, $dN_1/dt = 0$. We then obtain Eq. 5 from Eq. 1:

$$\frac{N_2}{\tau_{21}} + W_s (N_2 - N_1) - W_p (N_1 - N_3) = 0. \quad (5)$$

Since the decay τ_{32} from state 3 to state 2 is very fast, we can consider all the atoms that have been pumped to the excited state 3 will immediately decay to state 2. Therefore the population N_3 in state 3 can be simply obtained by the Boltzman distribution:

$$N_3 = N_2 e^{-(E_3 - E_2)/kT} \equiv \beta N_2. \quad (6)$$

¹ Strictly speaking, n_{sp} should be calculated as $\frac{N_2}{N_2 - N_1 \frac{\sigma_a}{\sigma_e}}$, where σ_a and σ_e are the absorption

and emission cross-sections between state 2 and 1 respectively. In the case of Er^{3+} , $\frac{\sigma_a}{\sigma_e}$ is close

to 1 and will not change the principle of our discussions.

Substituting Eq. 6 into Eq. 5, we obtain the population inversion factor n_{sp} after some manipulation:

$$n_{sp} \equiv \frac{N_2}{N_2 - N_1} = \frac{W_p \tau_{21} + W_s \tau_{21}}{(1 - \beta) W_p \tau_{21} - 1}. \quad (7)$$

Therefore, n_{sp} is related to the pump and signal powers by W_p and W_s , respectively, and to the pump wavelengths by β . Eq. 7 has important implications both on amplifier gain and ASE (amplified spontaneous emission) noise as will be seen in the following sections.

It is worth mentioning here that for a four-level system, due to the fast decay from state 1 to state 0, the initial population at state 1 is very small and full population inversion ($n_{sp} = 1$) can be easily achieved even under weak pumping. Unfortunately, this is not the case for EDFAs.

2.2 Gain Spectrum and Gain Saturation

Optical pumping provides the necessary population inversion between the energy states 1 and 2, which in turn provides the optical gain defined as $g = \sigma(N_2 - N_1)$, where σ is the transition cross-section. Unlike that of an ideal homogeneously broadened gain medium, the gain spectrum of EDFAs (Fig. 2) is broadened considerably by the amorphous nature of silica and by the presence of other co-dopants such as germania and alumina within the fiber core, an advantage for WDM applications.

The gain coefficient decreases as the signal power level increases—a common phenomenon in laser and amplifier systems called *gain saturation*. This is a result of the

depopulation of state 2 due to an increasing number of signal photons. In fact, the gain coefficient can be written as [9]

$$g = \frac{g_0}{1 + P/P_s}, \quad (8)$$

where g_0 is the small-signal gain coefficient at a given wavelength,

P is the signal power, and

P_s is the saturated signal power, defined as the power required for the gain to drop 3dB.

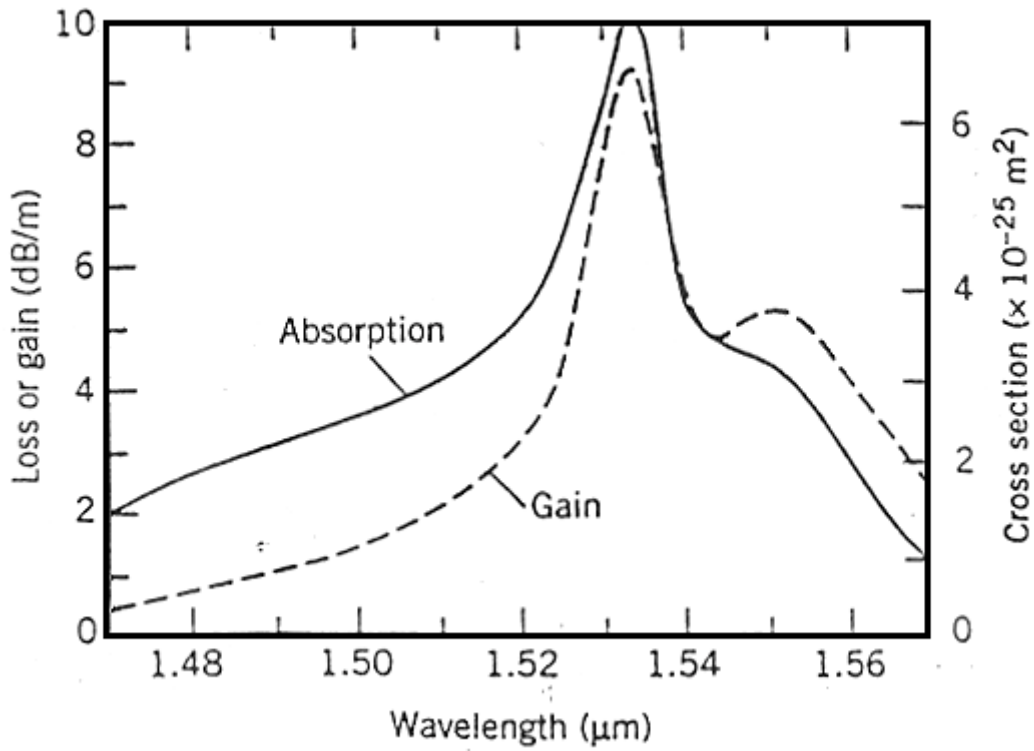


Fig. 2. Absorption and gain spectra of an EDFA whose core was co-doped with germania. (After Ref. 2)

The evolution of the signal power along the fiber can then be expressed as

$$\frac{dP}{dz} = g(z)P(z) = \frac{g_0(z)P(z)}{1 + P(z)/P_s}, \quad (9)$$

which can be easily integrated over the amplifier length [9] and the output signal power is

$$P_{out} = P(L) = GP_{in}, \quad (10)$$

where the amplifier gain G is implicitly given by

$$G = G_0 \exp\left(-\frac{G-1}{G} \frac{P_{out}}{P_{in}}\right),$$

and where G_0 is the unsaturated amplifier gain

$$G_0 = \exp\left(\int_0^L g_0(z) dz\right).$$

The noise characteristics under unsaturated and saturated conditions are different as will be seen in Section 3.3.

2.3 Pump Wavelength and Absorption Spectrum

Figure 3a shows the energy-state diagram of erbium ions (Er^{3+}) and Figure 3b shows the corresponding absorption spectrum. There are several states to which the erbium ions could be pumped, however, to be practical in real lightwave networks, the pump wavelength must be one that is available with high-power semiconductor diode lasers. Although there are existing laser diodes operating at 800 nm, 980 nm and 1480 nm, the pumping efficiency is low at 800 nm due

to excited-state absorption. The only pump wavelengths used in practical systems are 980 nm by strained-layer quantum well lasers based on GaAs and around 1480 nm by laser diodes based on InGaAsP.

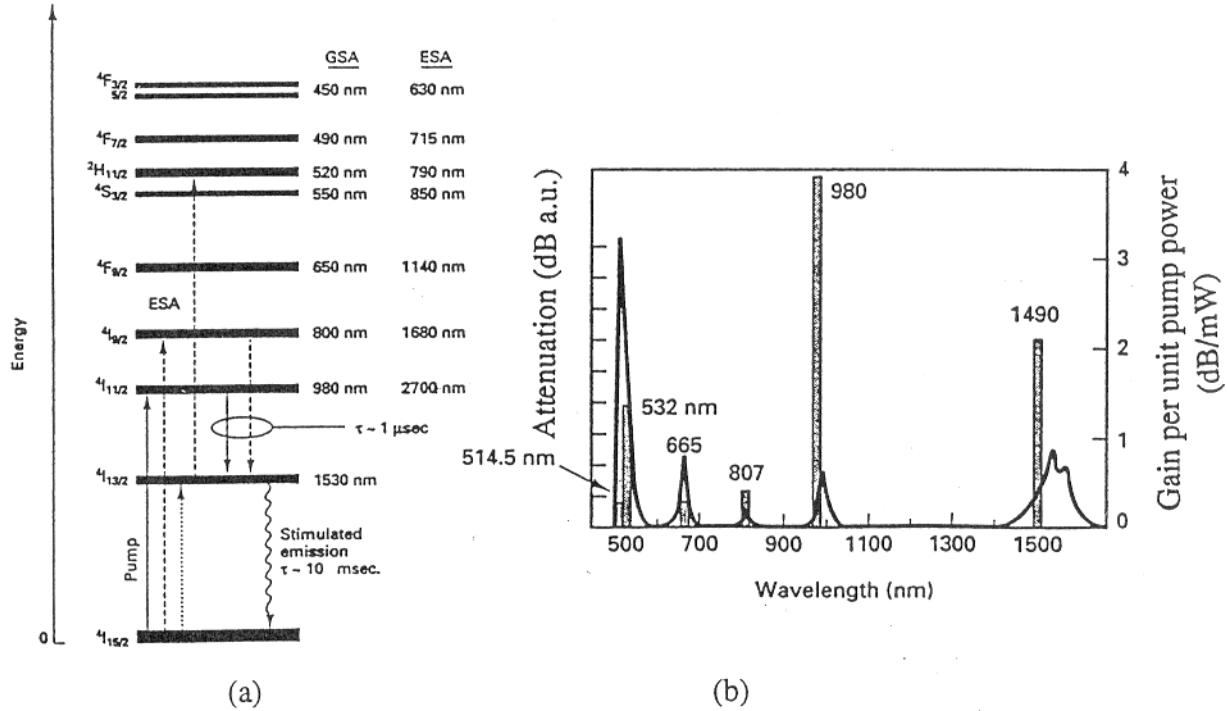


Fig. 3. (a) Energy levels of the triply ionized erbium ion, Er^{3+} . (b) Absorption bands of Er^{3+} (solid lines) and the pump efficiency (vertical bars). [After Ref. 3].

For 980 nm pumping, the pump band (state 3) is much higher above state 2. The parameter β (defined in Eq. 6) in this case is effectively zero, whereas β corresponding to 1480 nm pumping is about 0.38. It is obvious from Eq. 7 that 980 nm pumping can achieve a higher degree of population inversion than 1480 nm pumping with all other conditions held constant. Under the conditions of strong pumping ($W_p \tau_{21} \gg 1$) and a small signal (W_s negligible), n_{sp} for 980 nm pumping can reach 1, i.e. full population inversion, whereas 1480 nm pumping would not achieve full population inversion with $n_{sp} = 1.6$ for the best situation. This has serious

implications on the noise performance of the amplifier system, as will be discussed in Section 3.2.

2.4 Device configurations

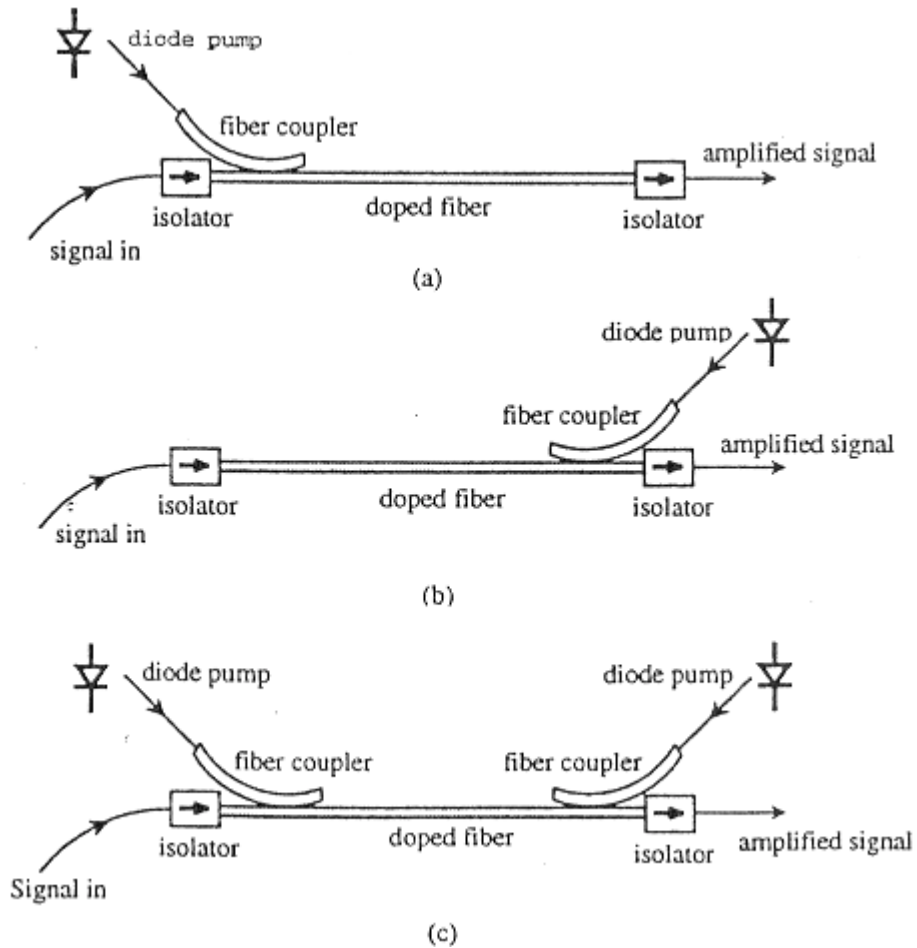


Fig. 4. Schematic of EDFA configurations utilizing (a) forward pumping (b) backward pumping and (c) both forward and backward pumping.

Figure 4 shows three EDFA device configurations. Pump beams are coupled into the doped fiber via the fiber coupler. Isolators are used at both ends of the fiber to avoid oscillation of the signal. Pump coupling can be in the forward direction (copropagating pump), the backward direction

(counterpropagating pump) or both directions (bidirectional pump). Forward pumping displays better noise performance than backward pumping, while backward pumping has the advantages of higher saturation power and higher gain. Bidirectional pumping has the merits of both at the cost of complexity.

3. Amplifier Noise

Now that we have an understanding of the underlying physics of optical amplification, we will proceed to exploring the noise characteristics in EDFA systems.

3.1 *The Quantum Limit*

As early as 1982, Carlton M. Caves[4] quantum mechanically proved that "a linear [phase-insensitive] amplifier *must* add noise to any signal it processes; the added noise must be *at least the* equivalent of doubling the zero-point noise associated with the input signal." In other words, a linear phase-insensitive² amplifier suffers at least a 3dB penalty on the signal-to-noise ratio (SNR).

R. Loudon[5] further calculated, using a quantum mechanical approach, the change of the means and variances of the electrical field E_0 and photon number n_0 of the input light by a linear amplifier in which the input light is coupled to an inverted atomic population, from which he derived the relations between the output SNR and the input SNR for both the electric field and the photon number [5]:

² A phase-insensitive amplifier takes no account of the phase of the input light. The inverted atomic population amplifier typifies a phase-insensitive amplifier. On the other hand, parametric amplifiers typify phase-sensitive amplifiers in that the amplification depends on the phase of the input. The 3dB penalty does not apply to phase-sensitive amplifiers.

$$\left(\frac{S}{N}\right)_{out} = \frac{G}{2n_{sp}(G-1)+1} \left(\frac{S}{N}\right)_{in} \quad (\text{field}) \quad (11)$$

$$\left(\frac{S}{N}\right)_{out} = \frac{G^2 \langle n_0 \rangle}{n_{sp}^2 (G-1)^2 + n_{sp} (G-1) + 2n_{sp} (G-1)G \langle n_0 \rangle + G \langle n_0 \rangle} \left(\frac{S}{N}\right)_{in} \quad (\text{number}) \quad (12)$$

where G is the amplifier gain and n_{sp} is the population inversion factor, both defined in the previous section.

The SNR given by Eq. 11 is important for assessing the effect of the amplifier in a coherent detection system, while the SNR given by Eq. 12 is important for direct detection systems.

Eqs. 11 and 12 clearly indicate that the signal to noise ratio is directly related to the gain and the population inversion factor. The amplifier noise is at a minimum when full population inversion occurs ($n_{sp} = 1$). In fact, with high gain ($G \gg 1$) and a large input ($\langle n_0 \rangle \gg 1$) under the full population inversion condition, Eq. 12 reduces to

$$\left(\frac{S}{N}\right)_{out} = \frac{1}{2} \left(\frac{S}{N}\right)_{in}, \quad (13)$$

which is the quantum limit.

3.2 Amplified Spontaneous Emission Noise

The fact that noise is inherent in all amplification systems based on atomic population inversion can be understood by the physical picture of amplified spontaneous emission. The noise photons

emitted randomly by spontaneous decay of excited atoms are initially negligible compared to the stimulated emission due to the presence of a large amount of signal photons (stimulating photons). However, as the signal and noise propagate along the gain medium (the doped fiber in this case), the spontaneous emission, as well as the stimulated emission, is amplified. The higher the gain, the greater the ASE noise. It can be shown that the amount of noise power associated with a single mode within a bandwidth $d\nu$ is [6]:

$$\boxed{P_n = h\nu n_{sp} (G(\nu) - 1) d\nu}. \quad (14)$$

This again shows that the noise power is proportional to n_{sp} and gain (assume $G \gg 1$). A four-level system can easily achieve $n_{sp} = 1$ (best value) and therefore has better noise performance. For the three-level Er:doped fiber amplifier, $n_{sp} = 1$ can be achieved with strong pumping at 980 nm, but for 1480 nm pumping, the ASE noise is 1.6 times (2dB) worse (refer to Eq. 7 and Section 2.3). This is experimentally verified by the measurements done by Cavaciuti, et. al. [7].

3.3 Noise Figure

The amount of noise power (Eq. 14) alone does not give us information on the performance of the system. The ultimate limiting factor for the detection system is the signal-to-noise ratio. For this reason, it is the *noise figure* F_n that is commonly used for characterizing the noise performance of the amplification system, defined as

$$\boxed{F_n = \frac{SNR_{in}}{SNR_{out}}}. \quad (15)$$

A simple derivation for the noise figure of a single amplifier (Fig. 5) for a direct detection system is given here [8].

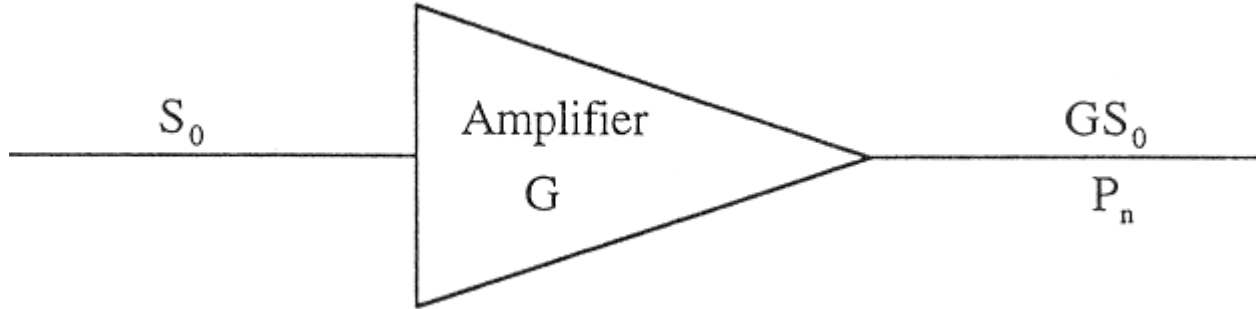


Fig.5. Optical amplifier with a power gain G and an input signal power S_0 . P_n is the total ASE power at the output of the amplifier in the appropriate bandwidth $\Delta\nu$. [After Ref. 8].

Consider a single optical fiber carrying an optical signal with power S_0 . The detected signal mean-square current is

$$\langle i_s^2 \rangle_{in} = \frac{S_0^2 e^2}{(h\nu)^2} \quad (16)$$

where e is the electronic charge, and we assume an optical modulation index of $m=1$ and a detector quantum efficiency of unity. The shot noise at the output of the detector is given by

$$\langle i_n^2 \rangle_{in} = \frac{2e^2 S_0 \Delta\nu}{h\nu} \quad (17)$$

so that the SNR power ratio at the input to the amplifier is then

$$SNR_{in} = \frac{\frac{S_0^2 e^2}{(h\nu)^2}}{\frac{(2e^2 S_0 \Delta\nu)}{h\nu}} = \frac{S_0}{2h\nu\Delta\nu} \quad (18)$$

The detected signal power at the output is

$$\langle i_s^2 \rangle_{out} = G^2 \frac{S_0^2 e^2}{(h\nu)^2} \quad (19)$$

while the corresponding shot noise is

$$\langle i_{shot}^2 \rangle_{out} = \frac{2e^2 G S_0 \Delta\nu}{h\nu} \quad (20)$$

In addition, there are two new sources of output noise current. The first is the current due to beating at the detector between the signal optical frequencies and the ASE frequencies. Such beating produces output noise current components in the same frequency range as that of the signal current. The mean-squared valued of this noise current, noting Eq. 14, is

$$\langle i_n^2 \rangle_{sig-ASE} = \frac{4e^2 G S_{out} P_n \Delta\nu}{(h\nu)^2} = \frac{4e^2 G S_0 (G-1) n_{sp} h\nu}{(h\nu)^2} \Delta\nu \quad (21)$$

The second noise current is due to the beating of ASE frequencies against themselves. This noise, which is proportional to P_n^2 , can be shown to be negligible if the signal power S_0 is not allowed to drop too far. The shot noise due to the ASE has been neglected, which is justified when $S_0 \gg P_n$. The SNR at the output of the amplifier is thus

$$SNR_{out} = \frac{\left(\frac{GS_0e}{h\nu}\right)^2}{\frac{2e^2GS_0}{h\nu}\Delta\nu + \frac{4e^2G(G-1)S_0n_{sp}\Delta\nu}{h\nu}} \quad (22)$$

where a 100% detector quantum efficiency is assumed. For large gain, $G \gg 1$, the second term in the denominator of Eq. 22 dominates, and

$$SNR_{out} \approx \frac{S_0}{4n_{sp}h\nu\Delta\nu} \quad (23)$$

The noise figure F_n , which is the ratio of the input SNR to the output SNR , is thus

$$F_n = \frac{SNR_{in}}{SNR_{out}} \approx 2n_{sp} \quad (24)$$

For the case of $n_{sp} = 1$, we have again reached the same conclusion of quantum limit as drawn by the quantum mechanical derivation by Loudon (Eq. 13).

Eq. 24 indicates that the noise figure depends solely upon the population inversion factor n_{sp} (averaged over the entire fiber amplifier length). As Eq. 7 indicates, n_{sp} is a function of pump and signal power, and exhibits different characteristics under saturated and unsaturated conditions. It is important to understand and predict the behavior of the noise figure under different conditions in order to design an optimized EDFA system.

3. Experimental Layout

Figure 6 shows the experimental layout. The pump is generated by a diode laser at 975.5 nm. The signal is from a tunable diode laser source with its output tuned to 1550 nm. Both pump and

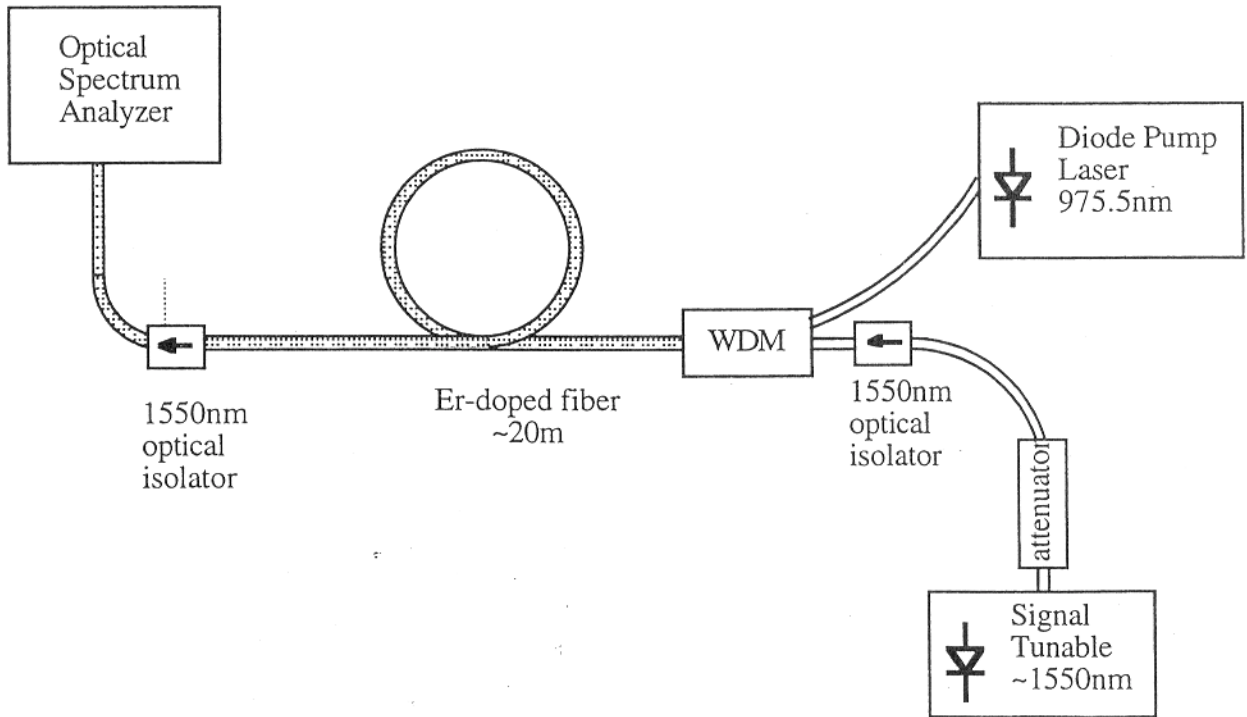


Fig. 6. EDFA layout.

signal are fiber coupled and are coupled into the Er-doped fiber by a wavelength division multiplexer (WDM). The attenuator is used to control the input signal power to the Er-doped fiber amplifier.

The construction of the EDFA is simple but requires careful handling of the fiber and couplers. After connecting the relevant fibers as illustrated in Fig. 6, we proceeded to take measurements.

4. Results and Discussions

1) ASE spectrum measurement

We set the pump diode current at the maximum allowed current, 175 mA, which corresponds to a pump power of 80.3 mW. With the signal diode current off, we measured the spectral output of the Er-doped fiber by the OSA, and thus obtained the ASE spectrum.

Figures 7a and 7b show the noise spectra of the EDFA on a dB and linear scale, respectively. The following parameters are obtained from the ASE spectrum graphs:

Peak frequency: 194.1005 THz

3dB bandwidth: 196.61 THz - 191.97 THz = 4.64 THz

Peak wavelength: 1544.1 nm

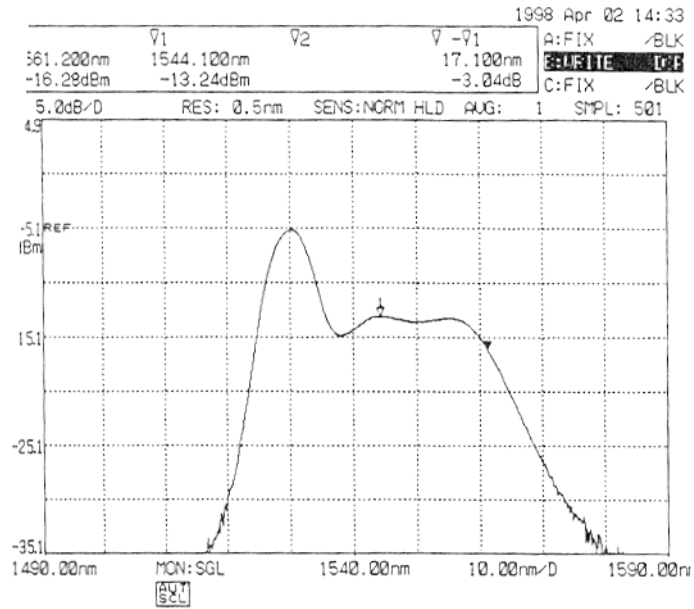
3dB bandwidth: 1561.2 nm - 1524.4 nm = 36.8 nm

2) Threshold pump power P_p^{th} measurement

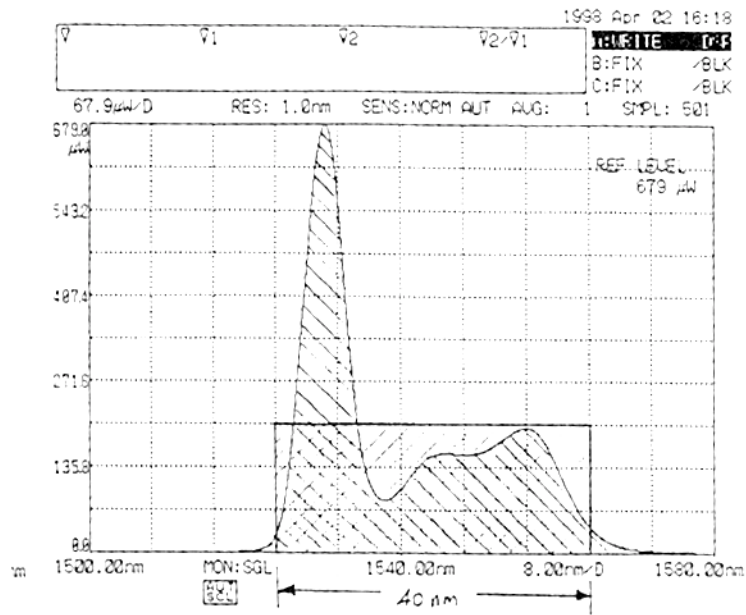
We set and held the input power at a constant value while varying the pump power and monitoring the output signal power using the OSA (Fig. 8). By comparing the peak output signal power with the peak input signal power stored in the OSA memory, we found the transparency point, where the pump power reaches the threshold, to be around 18.3 mW (Fig. 8b).

We further verified that the threshold pump power remains the same for different signal input levels. We first calibrated the signal input power with respect to the diode current supply:

	LD Current	Signal Peak Power Density (per 0.05 nm)
Signal 1	20.1 mA	-18.4 dBm
Signal 2	34.8 mA	-8.3 dBm



(a)



(b)

Fig. 7. ASE noise spectrum on different scales. (a) dB scale. (b) a linear scale.

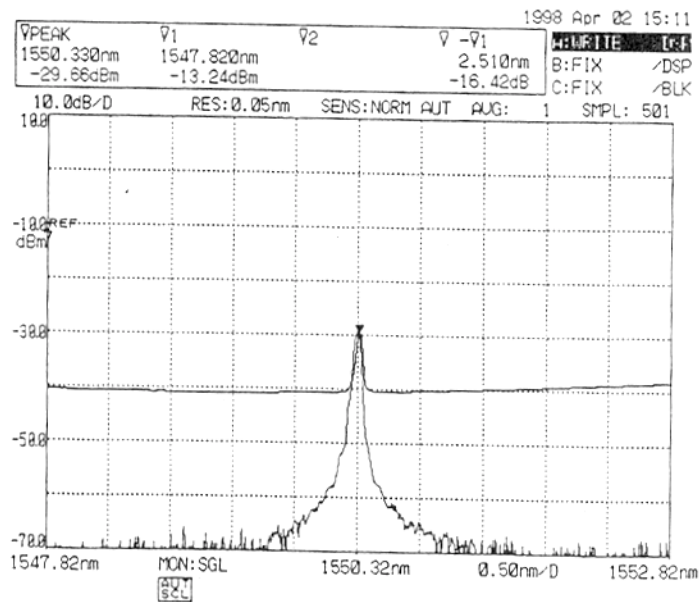
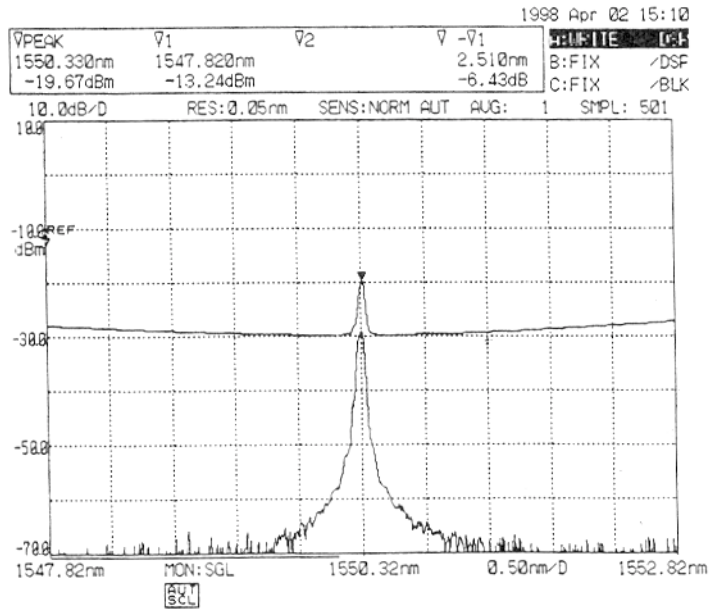


Fig. 8. Input and output signal spectra with pump power set at (a) 43.1 mW and (b) 18.3 mW.

We then repeated the procedure described above for different signal input levels. The results are tabulated here:

Table 1 Gain vs. pump power for two different signal input levels.

Pump Diode Current (mA)	Pump Power (mW)	Signal 1 Peak Power Density (dBm/0.05nm)	Gain 1 (dB)	Signal 2 Peak Power Density (dBm/0.05nm)	Gain 2 (dB)
175	80.31	-4.6	13.8	4.3	12.6
160	72.86	-5.1	13.3	4.0	12.3
145	65.41	-5.4	13.0	3.7	12.0
130	57.97	-5.9	12.5	3.0	11.3
115	50.52	-6.4	12.0	2.5	10.8
100	43.07	-7.2	11.2	1.5	9.8
90	38.11	-7.8	10.6	0.8	9.1
80	33.14	-8.7	9.7	0.2	8.5
70	28.18	-10.3	8.1	-1.7	6.6
60	23.21	-12.9	5.5	-4.2	4.1
55	20.73	-15.5	2.9	-6.1	2.2
51	18.74	-18.4	0.0	-8.4	-0.1
50	18.25	-18.5	-0.1	-9.1	-0.8
45	15.76	-23.3	-4.9	-14.1	-5.8

The threshold pump power in both cases is around 18.7 mW, which is consistent with the previous measured results within the error margin.

3) Gain vs. pump power and gain saturation

From the above measurement, we can plot gain versus pump power for the two input levels. Figure 9 shows that the gain coefficient decreases as the signal power level increases as a result of gain saturation.

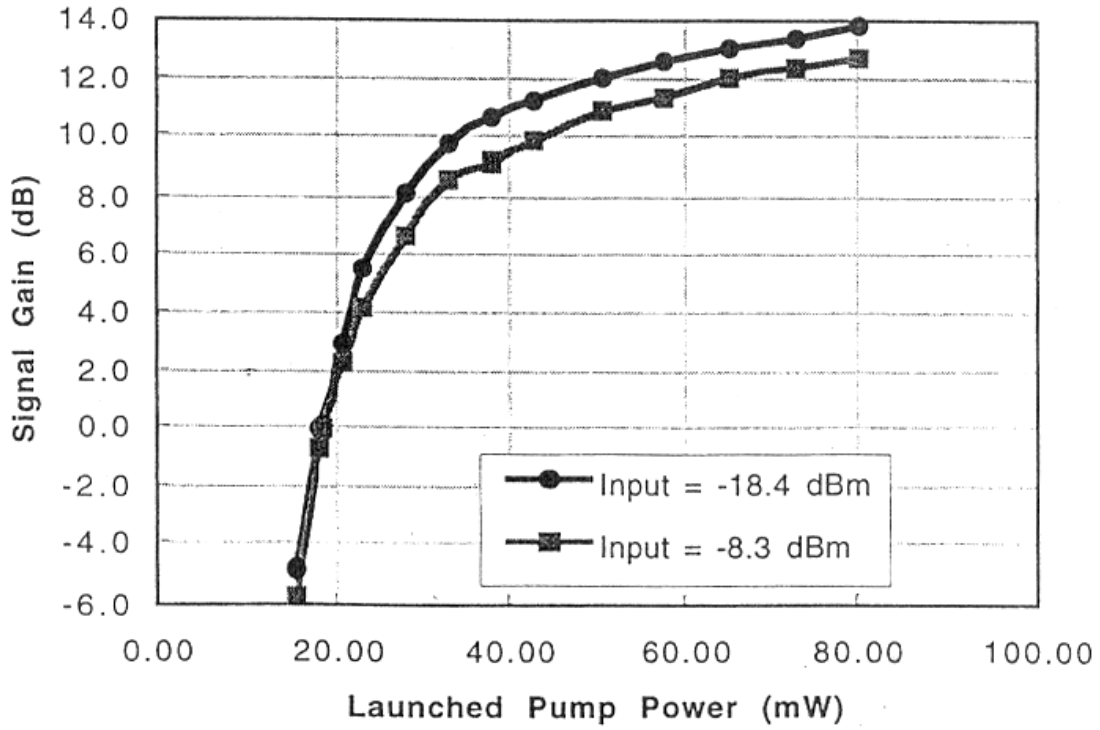


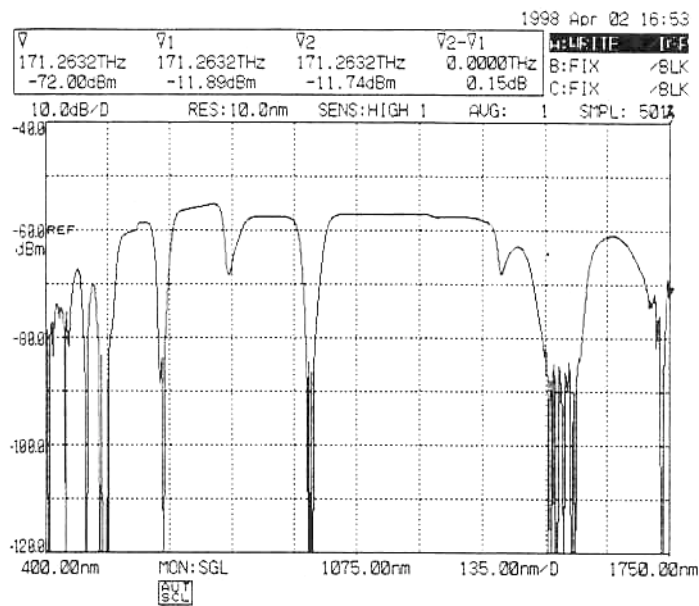
Fig. 9. Signal gain characteristics versus pump power.

Table 3 Population difference versus pump power.

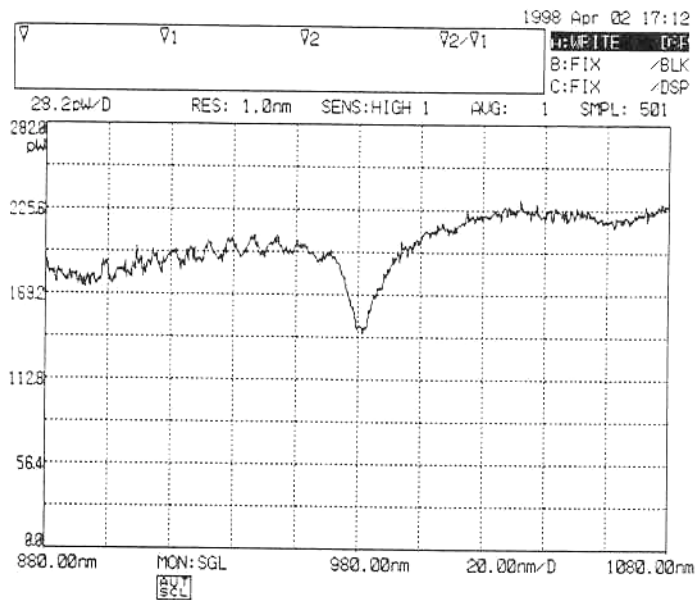
Pump Diode Current (mA)	Pump Power (mW)	Output Signal Power (dBm)	$N_2 - N_1$ (cm ⁻³)
175	80.31	-5.5	1.68 E+21
160	72.86	-5.6	1.67 E+21
145	65.41	-6.1	1.60 E+21
130	57.97	-6.3	1.57 E+21
115	50.52	-6.9	1.50 E+21
100	43.07	-7.5	1.42 E+21
90	38.11	-8.4	1.30 E+21
80	33.14	-9.3	1.18 E+21
70	28.18	-10.6	1.01 E+21
60	23.21	-13.4	6.50 E+20
55	20.73	-15.8	3.38 E+20
50	18.25	-19.2	-1.04 E+20
40	13.28	-31.0	-1.64 E+21
30	8.32	-48.5	-3.92 E+21
25	5.83	-59.6	-5.36 E+21

4. Absorption spectra for two different types of Er-doped fiber

The absorption spectra for two different types of Er-doped fiber were measured with a white light source. Fig. 10 (a) shows the spectrum for a 20-m sample of the same type of fiber as used in the EDFA experiment, with its horizontal scale expanded around 980 nm as shown in Fig. 10 (b). This fiber shows a series of absorption dips that correspond well with those shown in Fig. 3. On the other hand, Fig. 11 (a) shows a very different spectrum of another type of fiber of length 1 m. In particular, this fiber does not have a 1480 nm absorption dip at (Fig. 11 (b) cannot be pumped at 1480 nm).

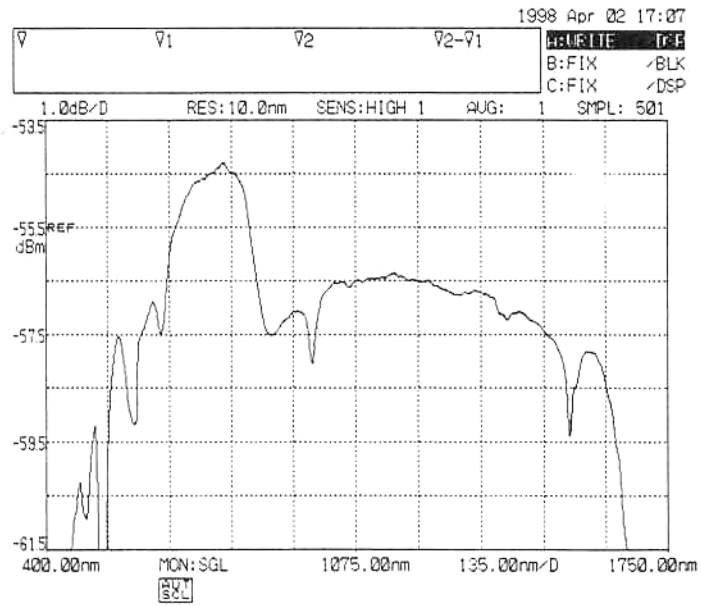


(a)

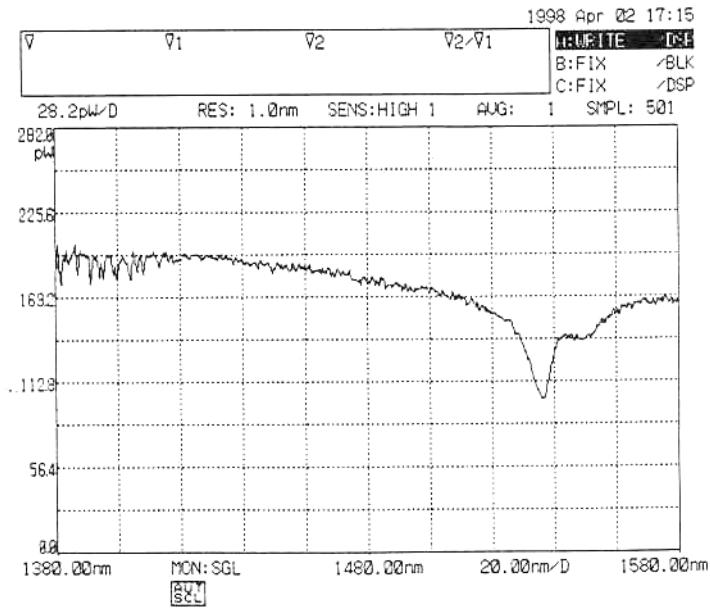


(b)

Fig. 10. Absorption spectrum of the 20-m fiber for (a) 400 nm –1750 nm, and (b) expanded around 980 nm.



(a)



(b)

Fig. 11. Absorption spectrum of the 1-m fiber for (a) 400 nm –1750 nm, and (b) expanded around 1480 nm.

5. Conversion efficiency η

The conversion efficiency is defined as the ratio of the signal power converted from the pump wavelength over the pump input power. We will calculate the conversion efficiency for the case where the peak input power is held at -18.4 dBm (assuming the signal has a FWHM of 0.05 nm) and the results are listed in Table 2.

Table 2 Calculated conversion efficiency for input peak power = -18.4 dBm.

Pump Diode Current (mA)	Pump Power (mW)	Output Signal Power (dBm)	η (%)
175	80.31	-5.5	0.33
160	72.86	-5.6	0.36
145	65.41	-6.1	0.35
130	57.97	-6.3	0.38
115	50.52	-6.9	0.38
100	43.07	-7.5	0.38
90	38.11	-8.4	0.34
80	33.14	-9.3	0.31
70	28.18	-10.6	0.26
60	23.21	-13.4	0.13
55	20.73	-15.8	0.06

For example, for the values given in the first row, the input pump power is 80.31 mW, the output signal power is -5.5 dBm = 0.2818 mW and the input signal is -18.4 dBm = 0.01445 mW and therefore,

$$\eta = \frac{0.2818 - 0.01445}{80.31} \times 100\% = 0.33\%$$

The theoretical maximum conversion efficiency is obtained when all the pump photons are converted into signal photons, and therefore,

$$\eta_{\max} = \frac{h\nu_s}{h\nu_p} = \frac{\lambda_p}{\lambda_s} = 63\%$$

The actual conversion efficiency is smaller than this theoretical value due to (1) coupling losses for both pump and signal, (2) the pump power is not 100% absorbed in the fiber, (3) some absorbed pump photons are used to amplify noise, (4) the pump and signal mode do not overlap 100%, and (5) not all the excited Er^{3+} go through radiative emission. Figure 12 plots the conversion efficiency versus pump power. There is a sharp rise with increasing pump powers at low powers, but as the gain saturates, the conversion efficiency begins to decrease.

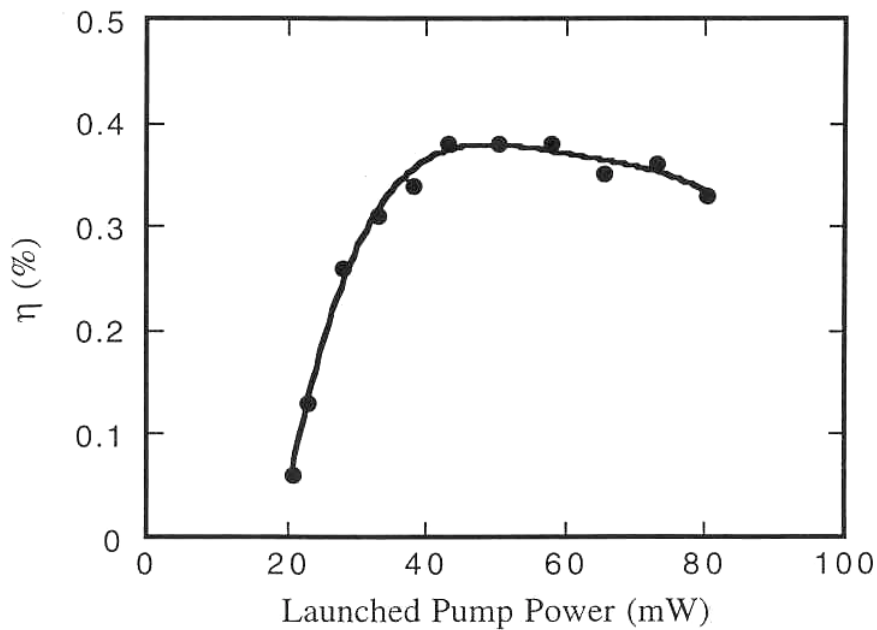


Fig. 12. Conversion efficiency of the EDFA as a function of pump power for a fixed input peak power of -18.4 dBm/0.05 nm.

6. Stimulated emission cross-section σ_s

The stimulated emission cross-section can be calculated as

$$\sigma_s = \frac{\lambda^2 g(\nu)}{8\pi n_1^2 \tau_{sp}} = \frac{\lambda^2}{8\pi n_1^2 \tau_{sp}} \frac{1}{\Delta\nu} \quad (26)$$

Here, $\Delta\nu$ is estimated from Fig. 7b. Since the absorption spectrum has an irregular shape, the 3 dB bandwidth is not a good estimate of $\Delta\nu$. Instead, we draw a box whose area is equal to the area under the absorption spectrum. We select the width of the box $\Delta\nu$ carefully so that the box has maximum area overlap with the absorption spectrum so that $\Delta\nu$ is most representative (Fig. 7 (b)). Thus, 40 nm is obtained as the bandwidth, which corresponds to $\Delta\nu = 5.03 \times 10^{12}$ Hz. Substituting this value into Eq. 26, we obtain

$$\sigma_s = \frac{\lambda^2 g(\nu)}{8\pi n_1^2 \tau_{sp}} = \frac{\lambda^2}{8\pi n_1^2 \tau_{sp}} \frac{1}{\Delta\nu} = \frac{(1.55 \times 10^{-6})^2}{8 \times 3.14 \times 1.46^2 \times 10 \times 10^{-3} \times 5.03 \times 10^{12}}$$

$$\sigma_s = 8.85 \times 10^{-25} m^2 = 8.85 \times 10^{-21} cm^2$$

The spontaneous lifetime of the ${}^4I_{13/2}$ level is taken to be 10 ms, an average value for most Er-doped fibers [3]. The calculated σ_s value is very close to what is reported in Ref. 3, indicating a simple way of calculating the emission cross-section by obtaining the emission spectrum.

7. Population Difference

To calculate the average population difference along the fiber, we need to know the average gain coefficient along the fiber from the overall gain

$$G = e^{gL} \quad 27$$

and then obtain the population difference from

$$g = \sigma_s (N_2 - N_1) \quad 28$$

Therefore,

$$N_2 - N_1 = \frac{g}{\sigma_s} = \frac{\ln G / L}{\sigma_s} \quad 29$$

where $L = 20 \text{ m}$ and $\sigma_s = 8.85 \times 10^{-21} \text{ cm}^2$ (calculated from above).

Table 3 tabulates the population difference versus pump power for a constant input signal power of -18.4 dBm . The negative values in Table 4 indicate $N_1 > N_2$, which is the case for pump powers below threshold. Instead of gain, we have absorption for these cases.

8. Calculated threshold pump power P_p^{th}

The pumping rate W_p at threshold can be obtained from Eq. 7 by considering $N_2 = N_1$ at threshold

$$W_p^{th} = \frac{1}{\tau_{sp}} \quad (30)$$

and W_p is proportional to the absorption cross-section σ_p at the pump wavelength and the pump photon flux density $\frac{I}{h\nu}$. For many types of fibers, σ_p ranges from 20×10^{-22} to $30 \times 10^{-22} \text{ cm}^2$ [3], except for Silicate L22 fiber. Here we will use an average value $25 \times 10^{-22} \text{ cm}^2$ since the exact type of the fiber we used is unknown. Therefore,

$$I_{th} = \frac{W_p^{th} h\nu}{\sigma_p} = \frac{h\nu}{\tau_{sp} \sigma_p} = \frac{6.63 \times 10^{-34} \times \frac{3 \times 10^8}{980 \times 10^{-9}}}{10 \times 10^{-3} \times 25 \times 10^{-26}}$$

$$I_{th} = 81.18 \times 10^6 \text{ W / m}^2 = 8.18 \text{ kW / cm}^2$$

From the threshold intensity I_{th} to threshold power P_{th} , we need to know the fiber core area A and the pump overlapping factor Γ . For a core radius of $2 \mu\text{m}$ and $\Gamma = 0.4$, we have

$$P_p^{th} = I_{th} \frac{A}{\Gamma} = I_{th} \frac{\pi r^2}{\Gamma}$$

$$P_p^{th} = 8.18 \times 10^3 \frac{3.14 \times (2 \times 10^{-4})^2}{0.4} = 0.0026 \text{ W} = 2.6 \text{ mW}$$

The calculated threshold pump power (2.6 mW) is almost an order of magnitude lower compared to the measured value (18.7 mW). However, we assumed that N_1 and N_2 remained constant for the entire fiber length (20m), which is not the case in practice, especially since we are using forward pumping instead of the bi-directional pumping scheme. The pump intensity drops exponentially with respect to fiber length, and at the ‘‘transparency point’’ measured in this

experiment, N_2 does not equal to N_1 for the entire fiber length. Instead, the signal experiences gain in the beginning of the fiber where $N_2 > N_1$ and loss at the end of the fiber where $N_2 < N_1$. Furthermore, there are coupling losses, which have not been taken into account during the calculation.

9) Noise power

Here we intend to verify Eq. 14 where n_{sp} , the population inversion factor, is expressed in Eq. 7. Again we assume W_p , W_s , N_2 , and N_1 are constant for the whole fiber length for ease of calculation, but this assumption can cause significant discrepancy between theory and measurement.

By substituting the following into Eq. 7 and 14

$$W_p = \sigma_p \frac{I}{h\nu_p} = \sigma_p \frac{P_p \Gamma_p}{A h \nu_p}$$

$$W_p = 25 \times 10^{-26} \frac{0.6 P_p}{3.14 (2 \times 10^{-6})^2 6.63 \times 10^{-34} \times 3.06 \times 10^{14}}$$

$$W_p = 5.88 \times 10^4 P_p$$

$$W_s = \sigma_s \frac{I}{h\nu_s} = \sigma_s \frac{P_s \Gamma_s}{A h \nu_s}$$

$$W_s = 8.85 \times 10^{-25} \frac{0.4 P_s}{3.14 (2 \times 10^{-6})^2 6.63 \times 10^{-34} \times 1.93 \times 10^{14}}$$

$$W_s = 2.20 \times 10^5 P_s$$

$$\tau_{21} = 10 \text{ ms}$$

$$\beta = 0$$

$$dv = 0.1 \text{ nm}$$

we calculate the noise power versus pump power and compare them with the measured values, as shown in Table 4.

Table 4 Comparison between the calculated and measured noise power.

Pump Power (mW)	Output Signal Power (mW)	n_{sp}	Calculated Noise Power (dBm)	Measured Noise Power (BW=0.1nm) (dBm)
80.31	0.282	1.04	-35.1	-17.5
72.86	0.275	1.04	-35.2	-17.9
65.41	0.245	1.04	-35.7	-18.4
57.97	0.234	1.05	-35.9	-19.1
50.52	0.204	1.05	-36.5	-19.9
43.07	0.178	1.06	-37.2	-21.0
38.11	0.145	1.06	-38.1	-22.0
33.14	0.117	1.07	-39.1	-23.4
28.18	0.087	1.08	-40.6	-25.2
23.21	0.046	1.09	-44.2	-28.6
20.73	0.026	1.09	-48.4	-31.7

The measured and calculated noise powers are plotted as a function of launched pump power in Fig. 13. There is a consistent 16 dB difference between the calculated noise power and the measured value. This large discrepancy can be partially explained by the rather unrealistic assumption we made for the calculation, that is, the pumping rate W_p stays constant throughout the fiber length. In fact, much of the pump power is lost during coupling and absorption. We

have probably over estimated W_p by an order of magnitude, as in the case for the pump threshold calculation.

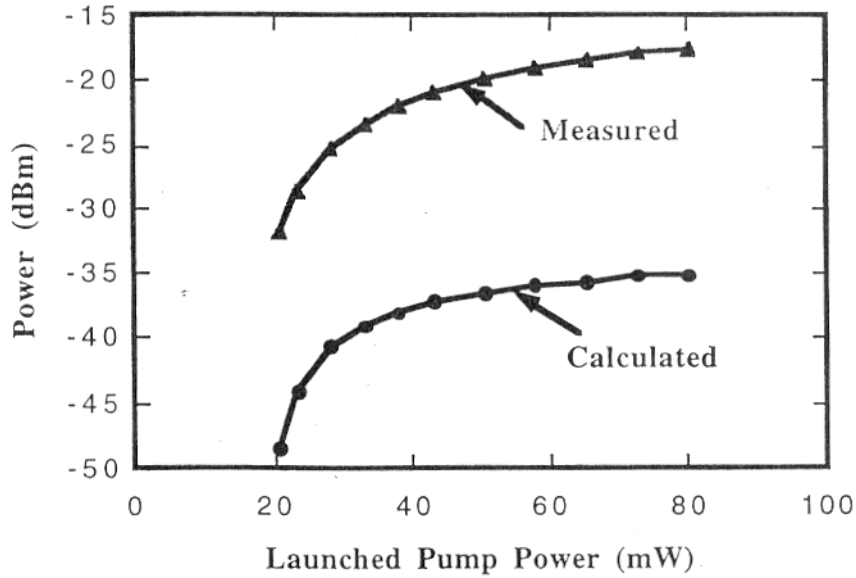


Fig. 13. Comparison between the measured and calculated noise power.

However, on the positive side, apart from the 16 dB offset, the measured noise power shows the same pump-power dependency as the calculated noise power, indicating a linear dependence on gain.

11) Construction of an EDF laser

An EDF laser can be constructed by connecting the erbium-doped fiber's output end to its input end and using the 980nm laser to serve as a pump laser. This configuration is shown in Fig. 14.

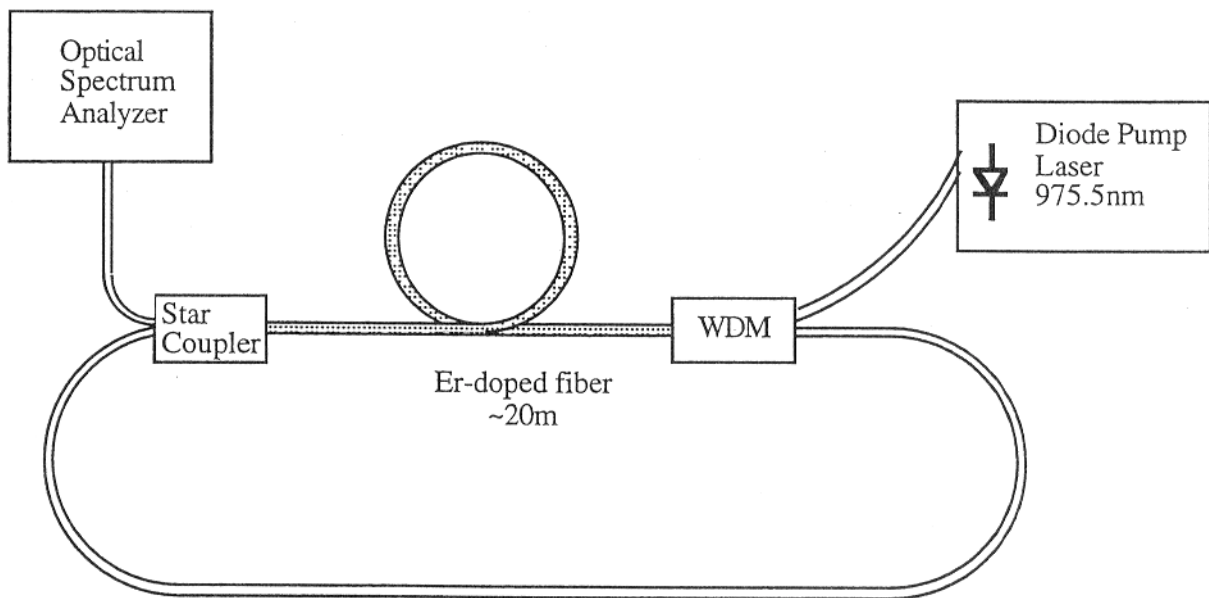


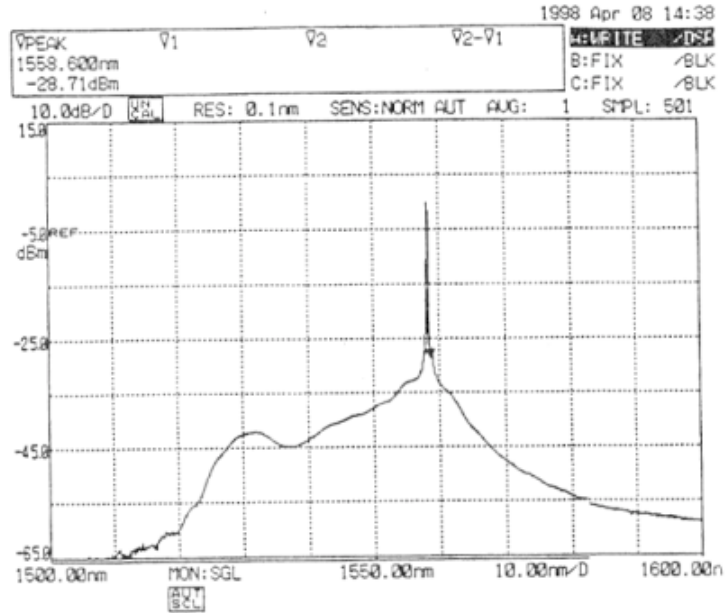
Fig. 14 Erbium-doped fiber laser layout.

The spectra of the laser is obtained by the OSA. Figure 15 shows a single lasing mode at the wavelength corresponding to the highest gain. Mode hopping, within a few nanometers of wavelength, is also observed without disturbing the fiber. Lasing is extremely sensitive, so much so that just touching the cavity fiber will cause lasing to fail. This shows that the EDF laser experiences high loss, possibly due to coupling loss, and any extra loss due to bending can stop the lasing. Multimode operation is also observed (Fig. 16) for bad fiber-to-fiber coupling, since significant coupling loss causes the laser to operate just above threshold.

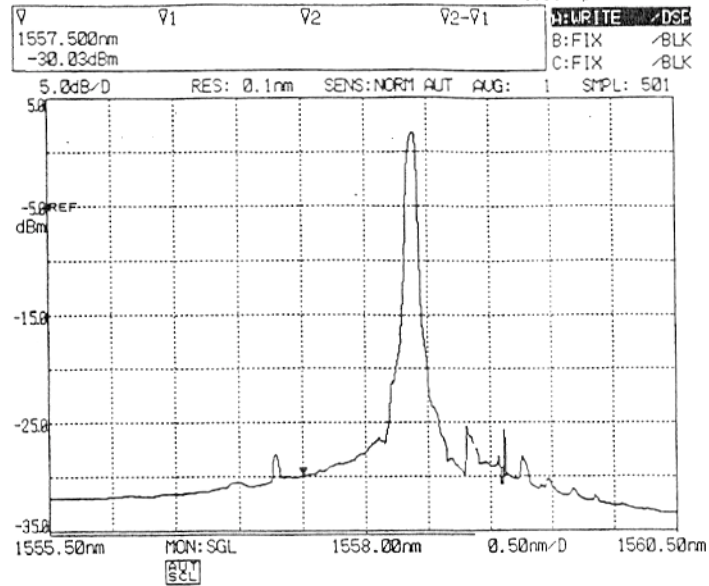
6. Conclusion

In this experiment, we have constructed an Er-doped fiber amplifier and have investigated many of its important parameters, including the ASE spectrum, the pump threshold power, the

emission cross-section, the conversion efficiency and the noise power dependency on pump power. We have shown that the emission cross-section for the 1550nm transition can be quite accurately calculated given the effective bandwidth of the ASE spectrum.



(a)



(b)

Fig. 15. Emission spectrum of the EDF laser using a 20-m fiber showing a single lasing mode in (a), and on an expanded scale in (b). The pump laser diode is set at 175 mA.

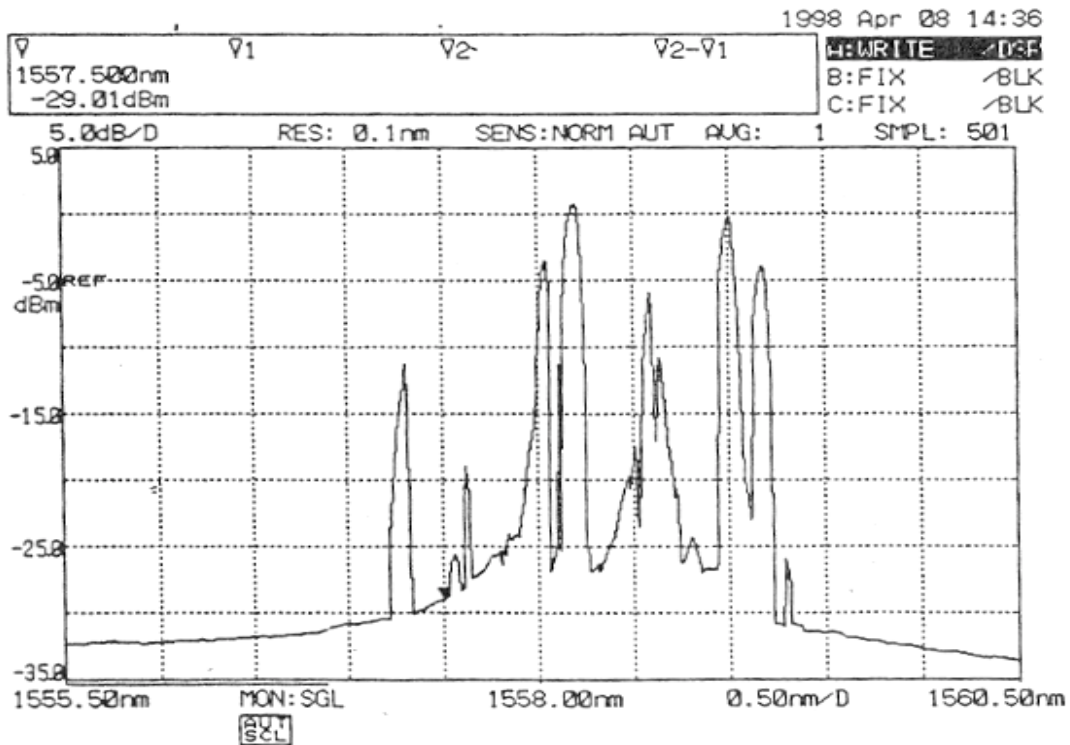


Fig. 16. Emission spectrum of the EDF laser using a 20-m fiber showing many lasing modes dues to bad coupling. The pump laser diode is set at 175 mA.

Our measurements on pump threshold power, conversion efficiency and noise power did not show good agreement with the theoretical calculation, mainly due to the large amount of coupling loss experienced in this experiment and the fact that we did not include the pump power variation along the fiber during our calculation.

An EDF laser was also constructed and its spectrum measured. Single mode operation can be obtained only for good coupling. In the case of bad coupling or bending introduced by tapping on the fiber, multimode operation or failure of lasing is observed. This shows that coupling losses play a significant role in the laser performance.

References

1. G. P. Agrawal, *Nonlinear Fiber Optics*, Section 11.1 (Academic Press, 1995).
2. C. R. Giles and E. Desurvire, *J. Lightwave Tech.* **9**, 271 (1991).
3. W. J. Miniscalco, "Erbium-doped glasses for fiber amplifiers at 1500 nm", *J. Lightwave Tech.* **9**, 234 (1991).
4. C. M. Caves, "Quantum limits on noise in linear amplifiers", *Phy. Rev. D.* **26**, 1817 (1982).
5. R. Loudon and T. J. Shepherd, "Properties of the optical quantum amplifier", *Optica Acta*, **31**, 1243 (1984).
6. A. Yariv, *Quantum Electronics*, 3rd ed. (John Wiley & Sons, 1989), Section 21. 1, p.572.
7. A. Cavaciuti, B. Sordo, "Noise measurements in EDFAs", Conference on Optical Fiber Communications, OFC'94 Technical Digest, paper WM9, 163 (1994).
8. A. Yariv, "Signal-to-noise considerations in fiber links with periodic or distributed optical amplification", *Opt. Lett.*, **15**, 1064 (1990).
9. K. Iizuka, Lab instruction notes for "Erbium Doped Fiber Amplifiers", University of Toronto, 1998.